Cancer Cell
Article

Kras^{G12D} and *Smad4/Dpc4* Haploinsufficiency Cooperate to Induce Mucinous Cystic Neoplasms and Invasive Adenocarcinoma of the Pancreas

Kamel Izeradjene,[1,3] Chelsea Combs,[4] Melissa Best,[1] Aarthi Gopinathan,[4] Amary Wagner,[4] William M. Grady,[1,3] Chu-Xia Deng,[5] Ralph H. Hruban,[6] N. Volkan Adsay,[7] David A. Tuveson,[4] and Sunil R. Hingorani[1,2,3,*]

[1] Clinical Research Division
[2] Public Health Sciences Division
Fred Hutchinson Cancer Research Center, Seattle, WA 98109, USA
[3] University of Washington School of Medicine, Seattle, WA 98109, USA
[4] Abramson Family Cancer Research Institute and Abramson Cancer Center, University of Pennsylvania School of Medicine, Philadelphia, PA 19104, USA
[5] Genetics of Development and Disease Branch, National Institute of Diabetes and Digestive and Kidney Diseases, National Institutes of Health, Bethesda, Maryland 20892, USA
[6] Departments of Pathology and Oncology, Sol Goldman Cancer Research Center, Johns Hopkins University School of Medicine, Baltimore, MD 21287, USA
[7] Department of Pathology, Harper Hospital and Wayne State University School of Medicine, Detroit, MI 48201, USA
*Correspondence: srh@fhcrc.org
DOI 10.1016/j.ccr.2007.01.017

SUMMARY

Oncogenic *Kras* initiates pancreatic tumorigenesis, while subsequent genetic events shape the resultant disease. We show here that concomitant expression of *Kras*^{G12D} and haploinsufficiency of the *Smad4/Dpc4* tumor suppressor gene engenders a distinct class of pancreatic tumors, mucinous cystic neoplasms (MCNs), which culminate in invasive ductal adenocarcinomas. Disease evolves along a progression scheme analogous to, but distinct from, the classical PanIN-to-ductal adenocarcinoma sequence, and also portends a markedly different prognosis. Progression of MCNs is accompanied by LOH of *Dpc4* and mutation of either *p53* or *p16*. Thus, these distinct phenotypic routes to invasive adenocarcinoma nevertheless share the same overall mutational spectra. Our findings suggest that the sequence, as well as the context, in which these critical mutations are acquired helps determine the ensuing pathology.

INTRODUCTION

Preinvasive neoplasms of the pancreas are among the most common and potentially lethal of the epithelial malignancies (Kozuka et al., 1979; Andea et al., 2003). These precursors to infiltrating pancreatic ductal adenocarcinomas (PDAs) typically progress through a series of histologically and genetically defined stages, collectively termed pancreatic intraepithelial neoplasias (PanINs). Resistant to all current forms of chemical and radiotherapies, PDA has a cumulative 5 year survival rate of less than 5% (Warshaw and Fernandez-del Castillo, 1992).

SIGNIFICANCE

Detecting preinvasive lesions and accurately determining their propensity for malignant transformation represent critical challenges for the practicing oncologist. For some malignancies, such as pancreatic cancer, resection at the preinvasive state may represent the only currently viable hope for cure. However, such interventions are not without risks or costs. Thus, determining when to intervene can be as important as the intervention itself. For cystic neoplasms of the pancreas, this diagnostic dilemma is particularly acute. Although less likely to transform and progress than their more classical intraepithelial counterparts, once cystic neoplasms have invaded and metastasized, they can be as lethal. We present here a genetically defined animal model of mucinous pancreatic cystic neoplasms that should enable detailed exploration of these critical issues.

Significant progress has been made in elucidating the genetic pathways to PDA (Hruban et al., 2000, 2001). Mutations in *KRAS* occur early in disease progression and are found in greater than 90% of invasive carcinomas; principal tumor suppressor gene mutations include *CDKN2A/INK4A* (95%), *TP53* (>75%), and *DPC4/SMAD4* (~55%). Systematic analysis of pathways of imputed importance in pancreatic oncogenesis can be accomplished by engineering these mutations individually, and in combination, into the laboratory mouse. Such experiments have established that endogenous $Kras^{G12D}$ expression can initiate pancreatic tumorigenesis and that the resultant preinvasive lesions progress to invasive and metastatic PDA (Hingorani et al., 2003). Concomitant $Kras^{G12D}$ and $Trp53^{R172H}$ expression results in accelerated development of PDA with clinical, histological, and genetic features that closely recapitulate those of the human disease (Hingorani et al., 2005). Disease is also hastened in the context of $p16^{Ink4a}$ deficiency (Bardeesy et al., 2006) and biallelic $p16^{Ink4a}/p19^{Arf}$ deletion (Aguirre et al., 2003), albeit with distinct clinical and histopathologic features. In each of these cases, however, abrogation of additional tumor suppressor gene pathways is not required, suggesting that there may be unique genetic routes to pancreatic cancer with corresponding and definable disease characteristics.

Distinct adenoma-to-carcinoma sequences exist in the pancreas in which invasive adenocarcinomas arise from cystic neoplasia (reviewed in Adsay, 2005; Hruban, 2006). Although the majority of cystic lesions in the pancreas are benign, a significant fraction represent preinvasive or focally invasive neoplasms, and with the advent and wider use of increasingly sophisticated imaging modalities, cystic neoplasms are being identified more frequently, often as incidental findings (Fernandez-del Castillo et al., 2003). Cystic neoplasms fall into two broad categories, intraductal papillary mucinous neoplasms (IPMNs) and mucinous cystic neoplasms (MCNs). Although several clearly distinct morphological and clinical criteria have been elaborated to distinguish these two categories of neoplasms (Hruban et al., 2004; Maitra et al., 2005), much less is known about the genetic events that underlie their formation and progression to invasive disease. When they do progress, IPMNs give rise most frequently to colloid carcinomas, but also to tubular (ductal) adenocarcinomas (Adsay et al., 2002). MCNs progress through preinvasive stages involving low-, moderate-, and high-grade dysplasia (or carcinoma in situ), culminating in invasive ductal adenocarcinomas. Thus, there appear to be multiple distinct histological as well as genetic trajectories for the evolution of neoplastic events in the ductal epithelium of the pancreas.

Intriguingly, the available data suggest that the overall profile of genetic events found in the development and progression of MCNs is highly congruous with that seen in the more conventional PanIN-to-PDA sequence. Nevertheless, resection of invasive carcinomas associated with MCNs portends a dramatically more favorable prognosis, with long-term survival rates of 50%–60% (Hruban, 2006). The reasons for the stark differences in histopathology and clinical behavior are unclear but are of obvious potential importance for the management of each entity.

We present here an exploration of the effects of disrupted TGFβ signaling on shaping disease initiated by $Kras^{G12D}$. We find that concomitant heterozygous deletion of *Smad4/Dpc4* in the murine pancreas results in the elaboration of macroscopic MCNs that closely resemble the human disease. In addition to elucidating key features of this challenging class of pancreatic cystic neoplasms and providing a means to probe the mechanisms underlying their distinctive properties, the findings also help illuminate general principles about the divergent pathogenetic routes to invasive ductal adenocarcinoma of the pancreas.

RESULTS

Targeting $Kras^{G12D}$ and *Smad4/Dpc4* Deletion to the Murine Pancreas

Previous studies involving constitutive heterozygous deletion of *Smad4* revealed no overt pathology in the pancreas (Takaku et al., 1998, 1999; Xu et al., 2000). We too found that targeted heterozygous or homozygous deletion of *Smad4/Dpc4* in the murine pancreas did not disrupt normal pancreatic development or alter parenchymal architecture (Figure S1 in the Supplemental Data available with this article online). Moreover, $Dpc4^{flox/+}$*;Cre* and $Dpc4^{flox/flox}$*;Cre* animals did not manifest clinical signs of pancreatic insufficiency, had normal fasting blood glucose levels, gained weight normally (data not shown), and had a normal life span (see below). The synthetic functions of both the exocrine and endocrine compartments of the pancreas also appeared to be intact (Figure S1).

We surmised, therefore, that initiation of preinvasive disease in the pancreas would again require endogenous expression of oncogenic $Kras^{G12D}$ (Hingorani et al., 2003). We targeted oncogenic *Kras* expression and conditional *Smad4/Dpc4* deletion to progenitor cells of the murine pancreas using a strategy similar to that described previously (Figure 1A) (Hingorani et al., 2003, 2005). Deletion of exon 8 of the floxed *Smad4/Dpc4* allele results in a frameshift, rapid degradation of the truncated transcript, and no evidence of protein expression by immunoblot (Yang et al., 2002; and see below).

We first targeted the desired genetic events to *Pdx*-1-expressing cellular compartments. $Kras^{LSL\text{-}G12D/+}$*;* $Dpc4^{flox/+}$*;Pdx-Cre* animals had a median survival of approximately 8 months, significantly shorter than control animals. At necropsy, we found that these animals developed large, space-occupying gastric neoplasms that were the proximal cause of death (data not shown). Many of these gastric tumors were locally invasive and metastatic squamous cell carcinomas. Interestingly, while the pancreata from these animals manifested preinvasive (PanIN) lesions as expected, they also revealed a distinct class of macroscopic cystic lesions, primarily of the body

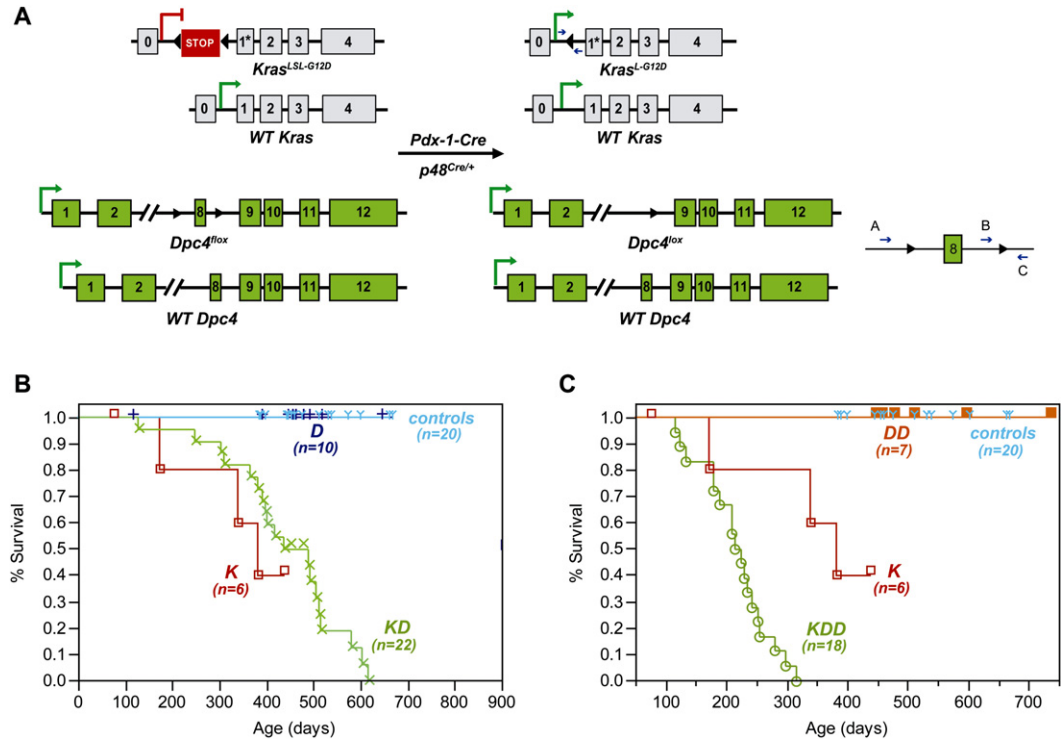

Figure 1. Targeting Endogenous *Kras*^{G12D} Expression and *Dpc4*/*Smad4* Deletion to the Mouse Pancreas

(A) Endogenous *Kras*$^{LSL\text{-}G12D/+}$ and *Dpc4*$^{flox/+}$ alleles are conditionally activated and deleted, respectively, upon tissue-specific exposure to *Cre* recombinase. Specific PCR analyses (inset, small blue arrows) permit genotyping of animals and detection of the respective "1LoxP" product after recombination of each targeted allele.

(B) Survival of *Kras*$^{LSL\text{-}G12D/+}$;*Dpc4*$^{flox/+}$;*p48*^{Cre} (*KD*) mice is significantly less than that of *Dpc4*$^{flox/+}$;*p48*^{Cre} (*D*) animals and of mice carrying only one or none of the various alleles (controls) ($p < 0.001$, log rank test, for each pairwise combination). Survival of *KD* animals is not significantly different from that of *Kras*$^{LSL\text{-}G12D/+}$;*p48*^{Cre} (*K*) mice.

(C) Survival of *Kras*$^{LSL\text{-}G12D/+}$;*Dpc4*$^{flox/flox}$;*p48*^{Cre} (*KDD*) mice (8 months) is significantly decreased compared to controls, *Dpc4*$^{flox/flox}$;*p48*^{Cre} (*DD*), *KD*, and *K* mice ($p < 0.001$, log rank test, for each pairwise combination).

and tail of the organ (discussed further below), which had not been seen in our prior models.

Concomitant *Kras*^{G12D} Expression and *Smad4*/*Dpc4* Haploinsufficiency Induce Pancreatic Cystic Neoplasms

The gastric tumors arising in *Kras*$^{LSL\text{-}G12D/+}$;*Dpc4*$^{flox/+}$;*Pdx-Cre* animals undoubtedly reflected the extrapancreatic expression of *Pdx-1* (Offield et al., 1996). We therefore targeted expression of the relevant mutant alleles to the *p48*-specific compartment, which is more tightly confined to the pancreas (Kawaguchi et al., 2002). *Kras*$^{LSL\text{-}G12D/+}$;*Dpc4*$^{flox/+}$;*p48*$^{Cre/+}$ (*KD*) animals also had a shortened life span compared with various controls, although median survival was not significantly different from that of *Kras*$^{LSL\text{-}G12D/+}$;*p48*$^{Cre/+}$ (*K*) mice (Figure 1B). In younger animals, the pancreatic parenchyma and associated synthetic functions of *KD* animals were largely preserved (Figure S1). As the animals aged, however, they frequently developed palpable, compressible masses, usually in the left lower quadrant of the abdomen (Figure 2C). At necropsy, *KD* mice did not manifest gastric pathology but instead had macroscopic, mucinous cystic lesions in the body and tail of the pancreas (Figures 2A–2E). These animals also manifested a lower overall burden of macroscopic metastatic disease than *Kras*$^{LSL\text{-}G12D/+}$;*Trp53*$^{LSL\text{-}R172H/+}$;*Cre* (*KP*) mice (Hingorani et al., 2005) (Table S1). The head of the pancreas in these animals was characteristically micronodular and sometimes contained firm masses, as can be seen with expression of activated *Kras* alone (Hingorani et al., 2003); occasionally, the pancreatic head also revealed small visible cystic lesions (Figure 2A) but typically did not contain the large, multilocular cysts encountered in the tail and body. Indeed, the latter cysts could be as large as 2–3 cm in diameter and yield up to several milliliters of fluid. The generally serous cystic fluid also occasionally contained hemorrhagic material and cellular debris (Figure 2E).

Histologic Progression of Murine MCNs

The pancreata from *KD* animals contained preinvasive lesions consistent with the murine PanIN (mPanIN) progression scheme (Hruban et al., 2006). Importantly, and as described in previous models (Hingorani et al., 2003, 2005), these mPanIN lesions did not involve the main pancreatic duct or large branches (Figure 2N), but rather

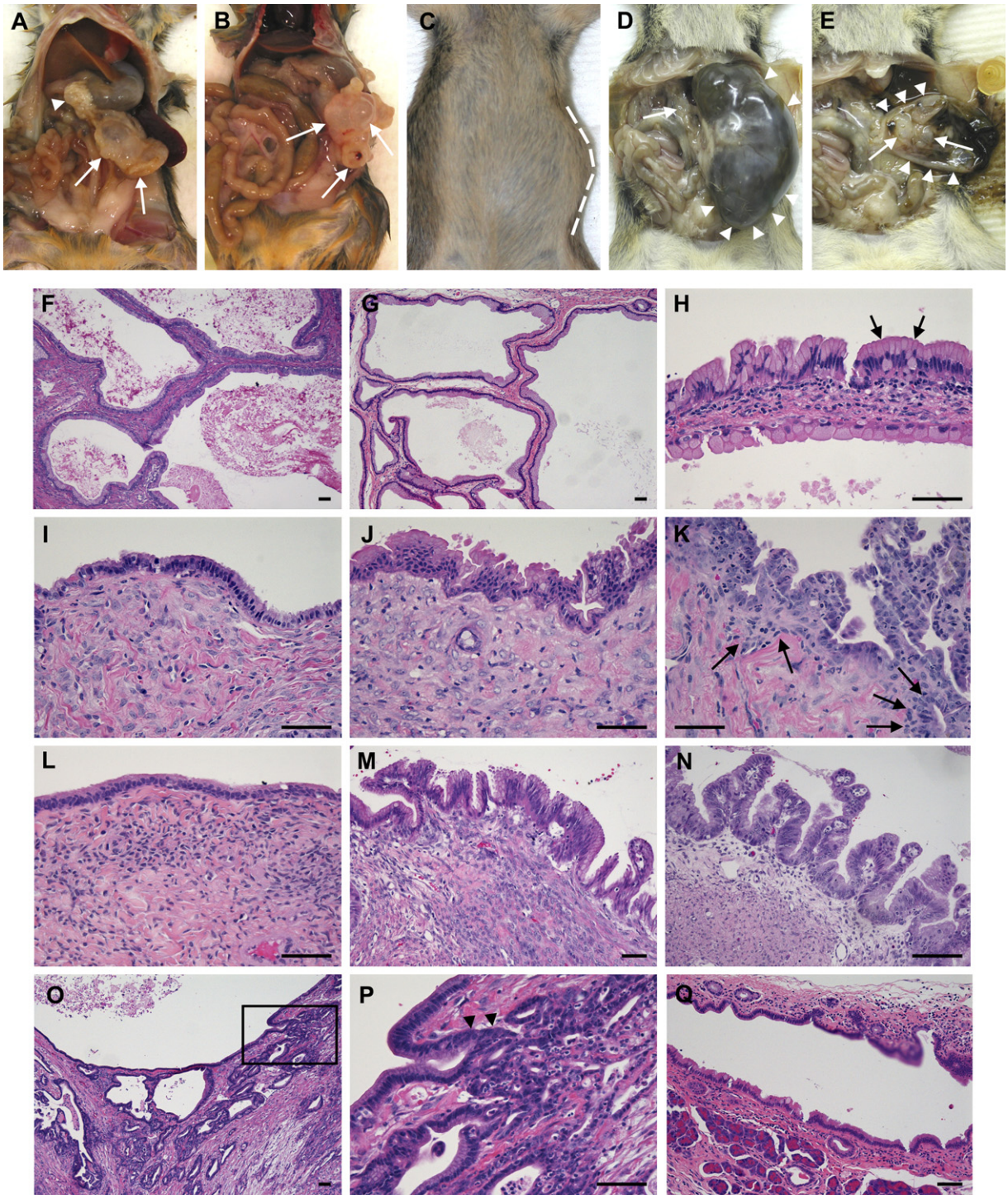

Figure 2. MCNs in *KD* Mice Faithfully Mimic the Human Disease

(A) Characteristic multilocular cystic lesion in the tail of the pancreas (arrows). The head of the pancreas in this animal also contained a small cyst (arrowhead).

(B) Multilocular cystic lesions (arrows) involving the body and tail of the pancreas.

(C) Palpable, compressible abdominal mass (dotted line) resulting from large hemorrhagic cyst in the tail of the pancreas (see [D] and [E]).

(D and E) Hemorrhagic cystic neoplasm ("chocolate cyst") in the tail of the pancreas before (D) and after (E) dissection. Note the thickened wall (arrowheads) and presence of nodules (arrows) within the cyst.

(F) Human MCNs revealing mucin-filled epithelial cell lining.

(G) Cluster of murine cystic lesions lined by mucinous columnar epithelium.

the peripheral ductules where human PanINs are also thought to originate. Interestingly, even by 7–8 months of age, the PanINs observed in *KD* animals were largely low grade; this contrasts with the significant numbers of PanIN-2 and high-grade PanIN-3 lesions that develop by this age in *Kras*$^{LSL\text{-}G12D/+}$;*p48*$^{Cre/+}$ littermates and in previously described *Kras*$^{LSL\text{-}G12D/+}$;*Cre* (Hingorani et al., 2003) and *KP* (Hingorani et al., 2005) mice. In addition to low-grade PanINs, cystic neoplasms were also noted microscopically throughout the *KD* pancreata, although they were particularly prominent in the body and tail of the organ. The cystic lesions were lined by columnar, mucin-filled epithelial cells (Figures 2G–2K) and also appeared not to involve the main pancreatic duct (Figure 2N), nor did they contain significant papillary projections into the lumen, which are more characteristic of IPMNs. The neoplasms showed nuclear and architectural evidence of progression from low-grade (Figures 2G–2I), to moderate (Figure 2J), to high-grade (Figure 2K) dysplasia. The surrounding stroma was frequently very cellular and contained spindle-shaped cells with distinctive ''wavy'' nuclei (Figures 2I–2K and see below), all features seen in human MCNs (Figures 2F, 2L, and 2M). Finally, the abundant mucin content of the cystic epithelium could be demonstrated by reaction with Alcian blue (Figure 3A), and the ductal phenotype of the epithelial cells was confirmed by expression of CK-19 (Figure 3B).

The stromal compartment of human MCNs characteristically demonstrates ''ovarian-type'' features, a reference to their compact growth pattern and wavy nuclei. These distinctive stromal elements are typically found in focal collections, usually in close association with the MCNs, and are notably not seen with IPMNs. The stromal cells also express characteristic markers, such as the progesterone receptor (PR) in 50%–75% of cases, and the estrogen receptor (ER) in approximately 25% of cases (Adsay, 2005). Many regions of the stroma in association with the mucinous cystic lesions of compound mutant animals possessed ''ovarian-like'' features (Figures 2I–2K and Figure 3). The stromal cells also showed strong nuclear expression of PR (Figure 3C) and, less frequently, ER (Figure 3D). In addition, spindle-like cells were also noted strongly expressing desmin (Figure 3E) and smooth muscle actin (Figure 3F), markers also found in the stroma of, though not specific for, MCNs in humans. We note that cystic lesions do also occasionally arise in previously described *Kras*$^{LSL\text{-}G12D/+}$;*Pdx-1-Cre* and *Kras*$^{LSL\text{-}G12D/+}$;*p48*$^{Cre/+}$ animals (Hingorani et al., 2003). Importantly, those cysts do not possess ovarian-like stroma, nor do the stromal cells express PR (Figure 3G) or ER (Figure 3H).

Attenuated Proliferation of Ductal Epithelium in MCNs

We have previously described the increased proliferation of ductal cells in PanIN lesions that occurs with endogenous *Kras*^{G12D} expression (Hingorani et al., 2003) and the intriguing apparent resistance of the acinar and islet cell compartments to such effects. The PanINs that develop in *KD* animals have a similarly elevated proliferative index as assessed by nuclear Ki-67 expression: 17.4% ± 0.6% of PanIN ductal cells express Ki-67, while less than 2% of acinar and 1% of islet cells are proliferating (Figure S3). Normal-appearing ductal cells in *KD* animals have a proliferative index of less than 0.3%, as was also found previously (Figure S3B). Intriguingly, although the ductal cells in MCNs demonstrated a higher proliferative index (2.0% ± 0.5%) than their normal counterparts (Figure S3C), this rate was nevertheless substantially attenuated as compared with cells in PanIN lesions. Thus, differentiation toward a cystic neoplasm may restrict the proliferative stimulus provided by oncogenic *Kras*. As the animals continue to age and the MCNs develop higher-grade dysplasia, their proliferative index also increases (10.4% ± 2.2%), particularly when found in association with invasive disease (Figure S3D).

Homozygous Deletion of *Smad4*/*Dpc4* Accelerates Development of MCNs

Kras$^{LSL\text{-}G12D/+}$;*Dpc4*$^{flox/flox}$;*p48*^{Cre} (*KDD*) animals succumbed earlier than their heterozygous counterparts (Figure 1C), with highly prevalent, macroscopic cystic lesions of the pancreas (Figure S2) similar to those described above, suggesting that LOH of *Dpc4*/*Smad4* contributes to disease progression (and see below). We note that both *KD* (median survival 15 months) and *KDD* animals (median survival 8 months) lived significantly longer than previously described *KP* mice (median survival 5 months; Hingorani et al., 2005). The latter cohort developed aggressive, locally invasive, and widely metastatic PDA highly reminiscent of human PDA. In contrast, the lesions in *KD* (Table S1) and *KDD* animals were less likely to invade or metastasize (Table S2). In particular, macroscopically evident metastases to the liver (35% and 18% versus 55%) and lung (18% and 0% versus 44%) were markedly less frequent in *KD* and *KDD* animals, respectively, as compared with *KP* mice (Hingorani et al.,

(H) Mucinous epithelia of adjacent cysts separated by a stromal septum demonstrating moderate-grade (top) and low-grade (bottom) dysplasia. Arrows indicate goblet-like cells.
(I) Cystic lesion with low-grade mucinous epithelium and surrounding highly cellular stroma. Note the dense growth and ''wavy'' nuclei of the stromal cells.
(J) Cystic lesion showing moderate atypia and surrounding highly cellular stromal compartment.
(K) Cystic lesion showing high-grade dysplasia with areas of focally invasive carcinoma (arrows).
(L–N) Human cystic neoplasms with low-grade (L), moderate-grade (M), and high-grade dysplasia (N).
(O and P) Invasive adenocarcinoma in association with cystic neoplasm at the tail of the pancreas. Note region of focal microscopic invasion extending from cyst to frankly invasive carcinoma ([O], box) and ([P], arrowheads).
(Q) Main pancreatic duct is characteristically uninvolved by preinvasive disease and appears histologically normal. Scale bars, 50 μm.

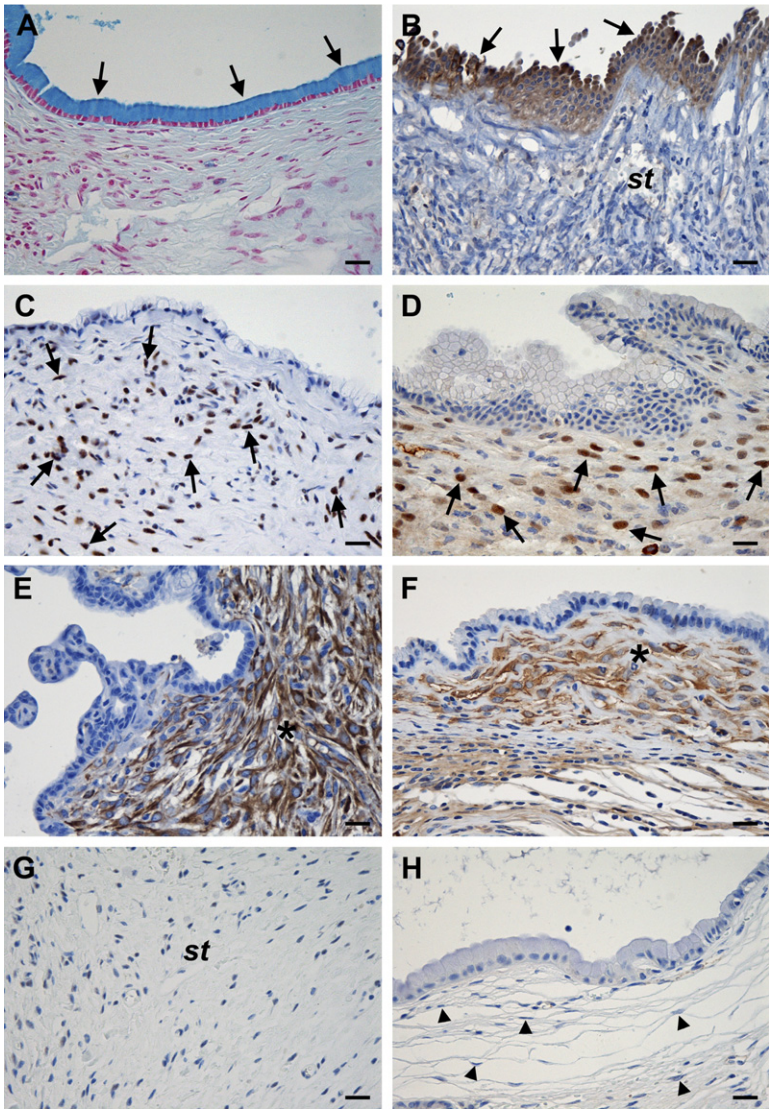

Figure 3. Characteristics of the Epithelial and Stromal Compartments of Murine MCNs

(A) Alcian blue stain revealing abundant apical mucin in cystic epithelial cells.

(B) Cytokeratin-19 expression in epithelial cells lining a cyst. *st*, highly cellular stroma underlying the cystic neoplasm.

(C and D) Nuclear expression of PR ([C], arrows) and ER ([D], arrows) in the stroma of distinct MCNs.

(E) Strong expression of desmin in stromal cells within a focus of invasion (asterisk).

(F) Stromal cells associated with an MCN expressing smooth muscle actin (asterisk). Note the wavy shape of the stromal nuclei.

(G and H) Lack of "ovarian-type" features and absence of PR (G) and ER (H) expression in the stromal cells (*st* and arrowheads) associated with a spontaneous cystic lesion arising in a *Kras*$^{LSL\text{-}G12D/+}$;*p48*^{Cre} animal. Scale bars, 20 μm.

2005). A lower propensity for invasion and metastasis is also seen with human MCNs as compared with ductal adenocarcinomas not arising in association with a cystic neoplasm.

Several criteria confirmed that the invasive lesions seen in the setting of the murine MCNs arose from the cystic neoplasms and not from the PanIN-PDA route. First, serial sectioning of the pancreata revealed multiple areas of direct microscopic invasion from MCNs into the surrounding parenchyma (Figures 2 and 4 and Figures S3 and S7). Second, the PanIN lesions in the adjacent parenchyma were invariably low grade (Figure S7). Third, although the metastatic lesions that developed in *KD* and *KDD* animals were clearly from ductal adenocarcinomas, they also reconstituted the cystic architecture of the primary lesions with striking fidelity, including demonstrating discrete stages of low, moderate, and high-grade atypia in the cystic epithelium (Figure S4). Metastases from the classical glandular PDAs that arise in *KP* mice similarly recapitulate the glandular features of their primary carcinomas (Figure S4 and Hingorani et al., 2005). Fourth, xenografts of primary cell lines derived from these invasive carcinomas also recapitulated both the glandular and cystic features of their origin (data not shown). Finally, the prolonged survival seen in these animals is consistent with the behavior of invasive adenocarcinomas arising from MCNs as opposed to PanINs, as is also found in patients. Collectively, the properties and histologic features of the murine cystic neoplasms described here faithfully recapitulate human MCNs. Although we considered the possibility that the lesions represent branch-duct IPMNs that have arisen in more distal portions of the ductal tree, the overall findings are more characteristic of MCNs (see below).

Signaling Pathways in Murine MCNs

A number of signaling pathways are aberrantly activated in human PanINs and PDA and similarly dysregulated in their murine counterparts (reviewed in Leach, 2004). Much less is known, however, about pathways and potential

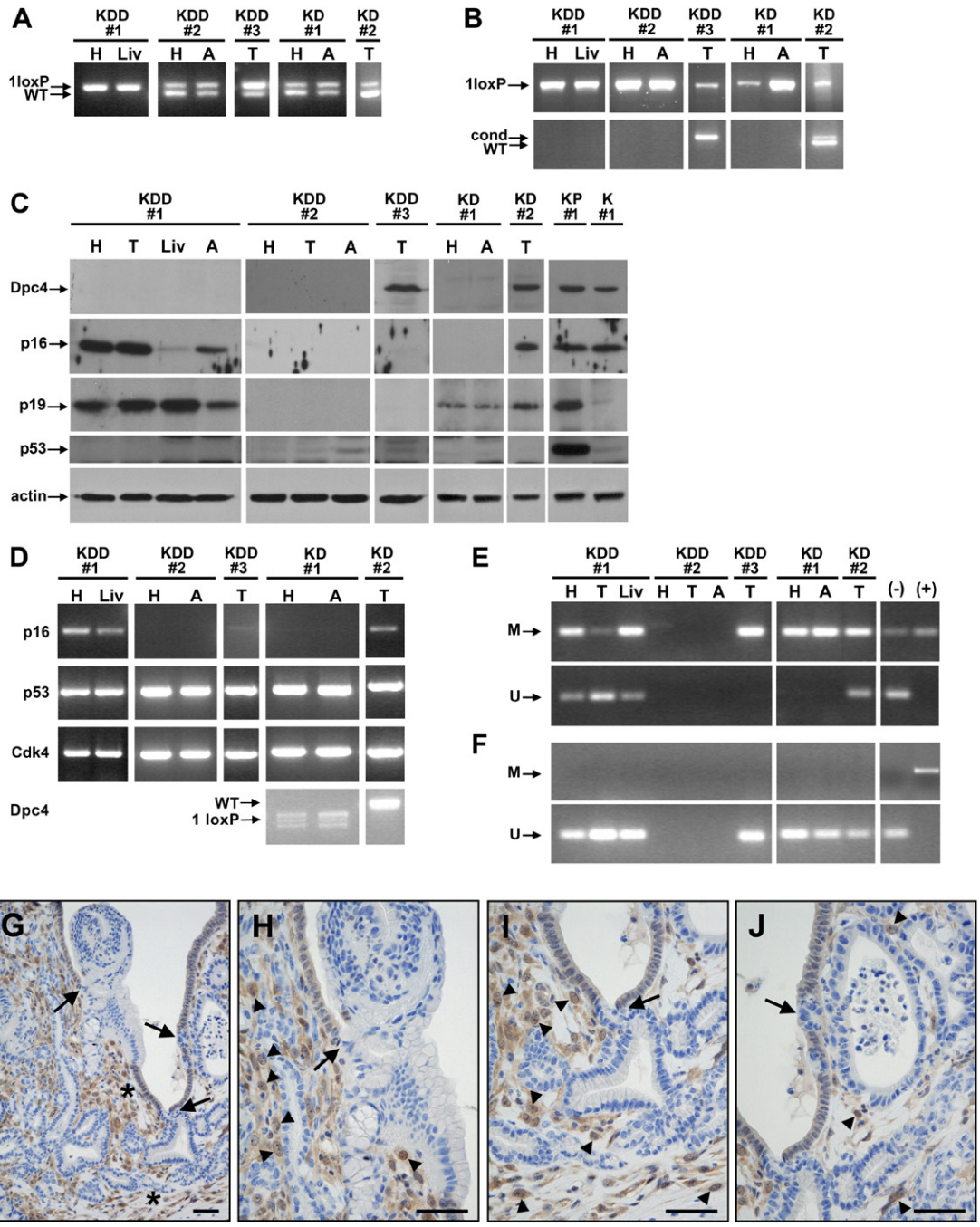

Figure 4. Molecular Characterization of Tumor Progression of Cystic Neoplasms in *KD* and *KDD* Animals

(A) Evidence of recombined *Kras* allele (1LoxP) in primary cell lines prepared from matched sets of pancreatic and metastatic tissues. WT, wild-type. Cell lines were prepared from the following tissues: H, head of pancreas; T, tail of pancreas; Liv, liver metastasis; A, ascites.

(B) A recombined *Dpc4* allele was detected in all primary cell lines (top panel). Distinct PCRs identify the recombined (1LoxP) as well as the conditional (cond) and wild-type (WT) alleles, respectively (see Figure 1).

(C) Immunoblot analyses of primary cell lines.

(D) RT-PCR analyses of indicated mRNAs in primary cell lines. Cell lines with complete recombination of conditional *Dpc4* allele show evidence of degraded transcript (e.g., *KD*#1), whereas those still retaining the *WT* and/or conditional (unrecombined) *Dpc4* allele preferentially reveal the full-length transcript by PCR of reverse-transcribed message (e.g., *KD*#2).

(E and F) Methylation-specific PCR of $p16^{Ink4a}$ (E) and $p19^{Arf}$ (F) loci in primary cell lines. (–), negative control DNA from normal murine colon (nevertheless demonstrates some methylation of *Ink4a* locus); (+), positive control from in vitro methylated DNA.

(G–J) Immunohistochemical analyses of Dpc4 in a murine MCN. Regions indicated by arrows in (G) are shown at higher power in (H)–(J). Note retention of Dpc4 in stromal cells (arrowheads). Scale bars, 50 μm.

therapeutic targets in cystic neoplasms of the pancreas. We therefore examined the expression of a number of receptors and signaling proteins in preinvasive, invasive, and metastatic cystic neoplasms of *KD* and *KDD* animals. *ErbB1* (*Egfr*) and *ErbB2* (*Her2/neu*) are upregulated in these murine MCNs and invasive carcinomas (Figure S5). High levels of Egfr expression persisted in invasive (Figure S5C) and metastatic lesions (data not shown), in contrast to the decreased expression that accompanied disease progression in *KP* animals (Hingorani et al., 2005). *Shh* was also consistently overexpressed, diminishing somewhat in metastases (Figures S5G–S5I). Strong pErk expression could be seen in dysplastic regions of the cystic epithelium, but not in regions retaining cuboidal morphology (Figures S5J and S5K). Robust expression could also be seen in invasive components but was typically restricted to the periphery of metastatic lesions (Figure S5L). Finally, Hes1, an indicator of Notch pathway activation, was aberrantly expressed in some, though not all, regions of dysplastic epithelium (Figure S5M); expression levels increased dramatically with the degree of dysplasia and persisted in invasive disease (Figures S5N and S5O). Thus, Hes1 may be a useful marker of more advanced disease. The level of Hes1 expression was also notably more marked than that in the previously described *Kras*$^{LSL\text{-}G12D/+}$; *Cre* model (Hingorani et al., 2003), perhaps reflecting a link between the TGFβ and Notch signaling pathways (Zavadil et al., 2004).

Genetic Progression of Murine MCNs

To attempt to define the additional genetic events required for progression of these murine MCNs, we isolated primary neoplastic cell lines from several pancreata and associated metastatic lesions by methods described previously (Hingorani et al., 2005). Matched portions of each resected specimen were processed in parallel for histologic and immunohistochemical analyses. Although it is formally possible that the isolated cell lines contain both preinvasive and invasive cells, as the cystic masses from which they were derived contained both preinvasive and invasive components, it was nevertheless clearly possible to discern critical genetic events associated with disease progression.

Several notable properties of the isolated primary cells were apparent. First, these neoplastic cell lines expanded more slowly than those from *KP* animals. Second, our overall success rate in establishing these lines (60%–70%) was lower than that of the previous model (>90%). Finally, these cells maintain a preference for growth on specialized substrates such as collagen, while *KP* cells are quickly able to grow equally well on plastic or collagen.

In a representative panel of primary cell lines isolated from *KD* and *KDD* animals, we characterized genetic events, transcript levels, and protein expression of several critical loci (Figure 4 and Table S3). We first confirmed that each of the isolated tumor cell lines contained the recombined oncogenic *Kras* allele (Figure 4A). Surprisingly, at least one matched set of primary pancreatic and liver metastasis cells (*KDD*#1) had also lost the wild-type *Kras* locus, suggesting the possibility that, in the setting of oncogenic *Kras*^{G12D}, the remaining wild-type allele may have a tumor-suppressive effect (Zhang et al., 2001). As expected, the floxed *Dpc4* allele was also recombined (i.e., deleted) and loss of the wild-type allele was observed in cells from several *Dpc4*$^{flox/+}$ mice (example *KD*#1, Figure 4B). There were rare instances of incomplete recombination of the *Dpc4* locus (see examples *KD*#2 and *KDD*#3, Figure 4B). *KD*#2 was derived from the pancreatic tail cyst shown in Figures 2D and 2E, histological analysis of which revealed the presence of a large cystic epithelial neoplasm in association with rare foci of microscopic invasion (data not shown).

Immunoblot analysis confirmed that Dpc4 expression was frequently lost in cells isolated from *KD* animals, consistent with LOH of this locus (Figure 4C). Many cell lines did not express p16^{Ink4a}, although they did usually retain expression of p19^{Arf}. The mechanism(s) by which these genes were effectively silenced was examined first by sequencing their respective cDNAs (see Experimental Procedures for details). The inability to isolate detectable message for *p16*^{Ink4a} and full-length message for *Dpc4* by RT-PCR from several of the lines explained their lack of protein expression (*KDD*#2 and *KD*#1, Figure 4D). The matched set of cell lines expressing high levels of p16 (*KDD*#1) had a uniform nonsense mutation in *Trp53*. Conversely, the samples that lacked significant p16 levels were found to have wild-type *Trp53*. Trp53 levels were induced by DNA damage in cells with wild-type *Trp53*, but not in those carrying mutant *Trp53*, confirming disruption of the pathway (Figure S6). No mutations were discovered in *Cdk4*, or in *Dpc4* when the full-length cDNA was recoverable.

The major mechanisms of *Cdkn2a/Ink4a* (*p16*^{Ink4a}) silencing in human pancreatic cancer include promoter methylation and deletion of the locus, with missense mutations being much less prevalent. Methylation-specific PCR (MSP) analyses revealed frequent methylation of the *p16*^{Ink4a} promoter region in primary tumor cell lines (Figure 4E). In some instances, only a methylated band was recovered, consistent with epigenetic silencing of expression (for example, *KD*#1, Figure 4E). We were unable to amplify the *Cdkn2a/Ink4a* locus at all in other cell lines (*KDD*#2-H, T and A, Figure 4E), providing an alternative mechanism for the loss of expression; specific PCR directed against another region of the locus gave the same result (data not shown). MSP for the *p19*^{Arf} locus, which is physically contiguous with that of *p16*^{Ink4a}, showed no evidence of methylation (Figure 4F). Thus, promoter methylation was specific for the *p16*^{Ink4a} locus, and *p16*^{Ink4a} expression was extinguished by a combination of epigenetic silencing and genomic deletion.

To confirm that LOH of *Dpc4* had occurred in vivo, and not as a result of the in vitro isolation of cell lines, we performed immunohistochemical analyses of resected tissue specimens. We found that Dpc4 expression was retained in preinvasive cystic neoplasms in *KD* animals, but lost in adjacent areas of invasive carcinoma and metastases (Figures 4G–4J, Figure S7, and data not shown).

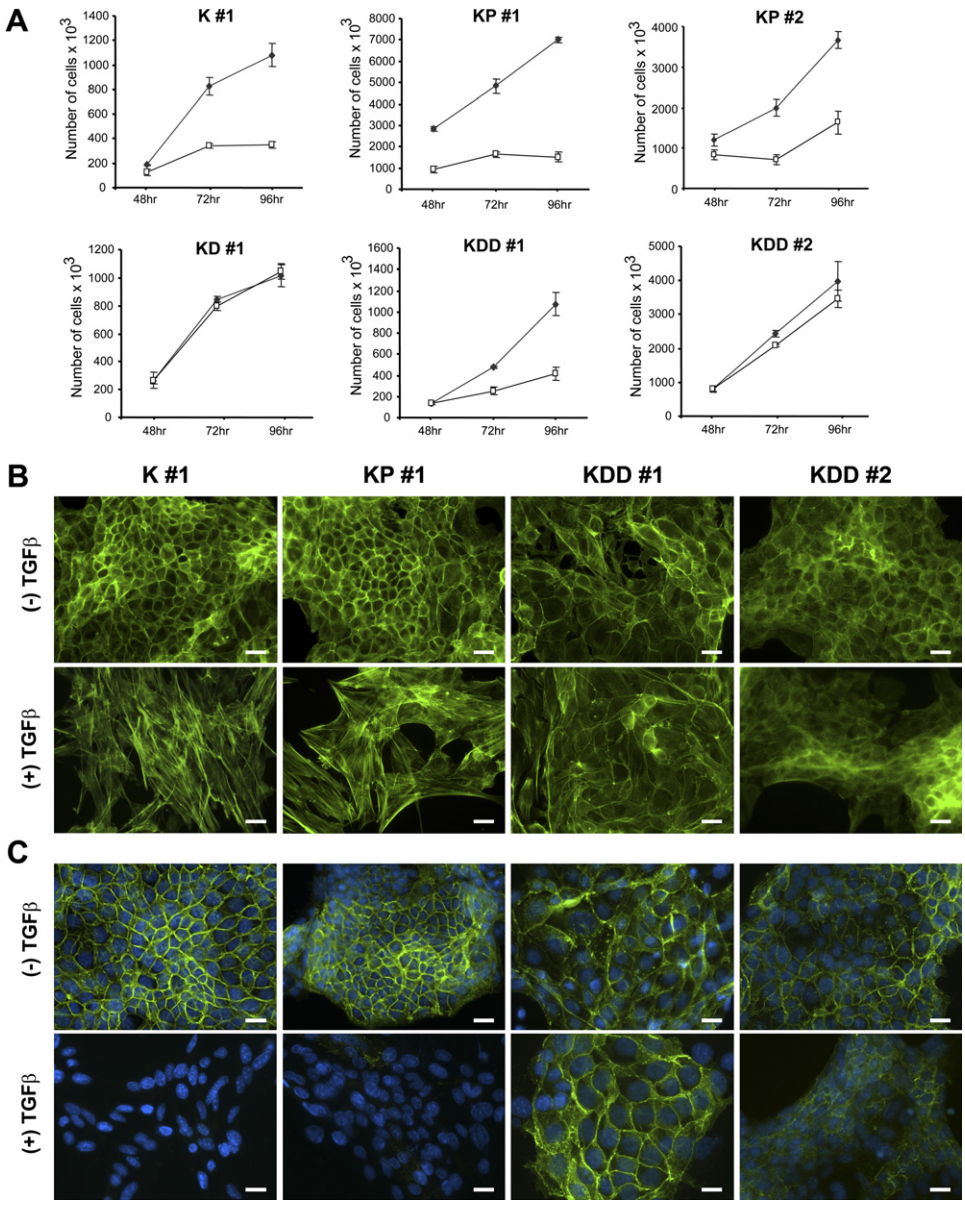

Figure 5. Effects of TGFβ on Cell Growth and Morphology

(A) Proliferation of primary cell lines in the presence (open symbols) or absence (closed symbols) of TGFβ.

(B and C) Induction of EMT by TGFβ requires *Dpc4*/*Smad4*. The presence of actin-stress fibers (B) and surface E-cadherin expression (C) were evaluated by reaction with phalloidin green and specific antibody, respectively. Cells were also stained with DAPI (blue). Scale bars, 20 μm.

Unfortunately, the available reagents do not permit similar studies for p16 with fidelity.

Finally, we performed measures of genomic instability in primary tumor cell lines derived from *KDD* mice. We had previously discovered a high degree of both numerical (simple) and structural (complex) genomic instability in the tumors and pancreatic cell lines from *KP* animals, processes that may have contributed to their highly invasive and metastatic nature (Hingorani et al., 2005). We found that centrosomal amplification, the presumptive proximal cause of losses and gains of whole chromosomes, was demonstrably less extensive in *KDD* cells than in *KP* cells (Figure S8). Preliminary analyses also revealed fewer nonreciprocal translocations, the hallmarks of complex chromosomal instability (data not shown). Interestingly, in *KDD* cells with a nonsense mutation in *Trp53*, the extent of centrosomal amplification was intermediate between that of *KDD* cells containing wild-type *Trp53* and *KP* ductal cells (Figure S8).

Smad4 Is Essential, but Not Sufficient, for Effective Growth Inhibition by TGFβ

To begin to elucidate the mechanistic basis for the unique phenotype observed in *Smad4*/*Dpc4* mutant animals,

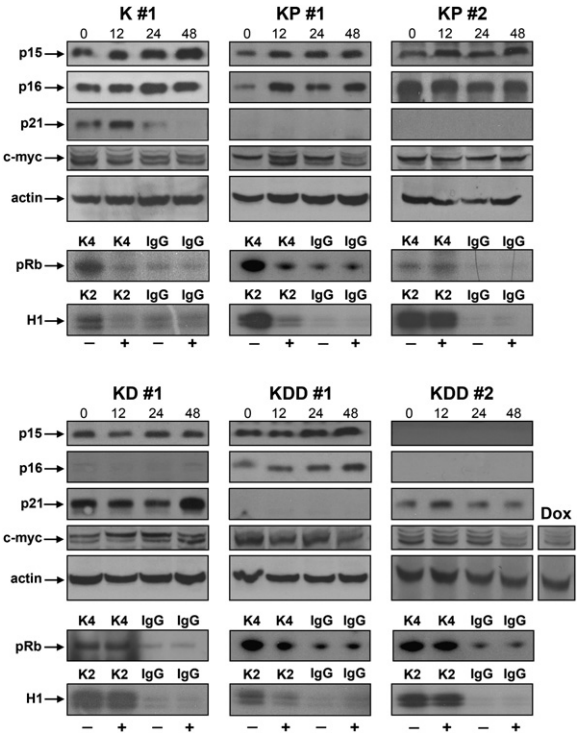

Figure 6. TGFβ Effects on the Expression and Activities of Cell-Cycle Regulators in Primary Ductal Cell Lines

Cells were treated with TGFβ for the indicated times (hr), and levels of p15, p16, p21, and c-*myc* were analyzed by immunoblot. The specificity of the c-*myc* band was confirmed by the known decrease in response to DNA-damaging agents such as doxorubicin (Dox). Cdk4 and Cdk2 kinase activities were measured in cells incubated with (+) or without (–) TGFβ; control assays were performed with rabbit serum (IgG).

we assessed the response of primary cells to TGFβ by several measures of neoplastic behavior. As expected, *Kras*$^{LSL\text{-}G12D/+}$;*p48*$^{Cre/+}$ pancreatic ductal cells (*K*#1) were efficiently growth arrested by TGFβ (Figure 5A). The proliferation of *KP* ductal cells was also significantly diminished by exposure to TGFβ, completely arresting growth in one cell line (*KP*#1) and slowing it in another (*KP*#2) (Figure 5A). Interestingly, neither *KDD* nor *KD* cells that had subsequently undergone LOH at the *Smad4*/*Dpc4* locus could be completely growth inhibited by TGFβ, although one cell line (*KDD*#1) was partially inhibited (Figure 5A). We note that the latter cells had elevated resting levels of both *p16*^{Ink4a} and *p19*^{Arf}, a possible compensatory result of the spontaneously acquired *Trp53* mutation. Similarly elevated levels of *p16*^{Ink4a} and *p19*^{Arf} are found in cell lines with engineered point mutation of *Trp53* (Figure 4 and Hingorani et al., 2005).

Not all *KP* ductal cells were susceptible to the growth effects of TGFβ (Figure S9A). As discussed further below, although these cells (*KP*#3) retained expression of key mediators of TGFβ effects, including *Smad4* and *p15*^{Ink4b}, the latter failed to be induced by TGFβ (Figure S9B). Thus, it appears that the ability of TGFβ to induce growth arrest in primary pancreatic ductal cells requires intact Smad4-mediated signaling in addition to other pathways (see below).

Induction of EMT and Enhanced Cell Migration Requires Intact *Smad4* Signaling

Epithelial-to-mesenchymal transition (EMT) denotes processes thought to be crucial for invasion and metastasis (Thiery, 2002). Members of the TGFβ superfamily, and principally TGFβ1, contribute to this transformation. We noted a dramatic induction of EMT by TGFβ in several *K* and *KP* ductal cell lines, manifested by a change from a discretely epithelial population of cells to one with the appearance of elongated, angular fibroblasts with projections and increased stress fiber formation (Figure 5B). Surface expression of E-cadherin also decreased notably in these cells (Figure 5C). TGFβ had markedly less pronounced effects on *KDD* ductal cells (Figures 5B and 5C), and on *KD* cells that had undergone LOH of *Smad4* (data not shown), suggesting that Smad4 may also be required for TGFβ-induced EMT.

We also measured the ability of cells to migrate across a wound in a monolayer. To distinguish the ability to complete wound closure by migration as opposed to proliferation, we incubated cells with TGFβ for 60 hr prior to wound induction to ensure sufficiently robust growth inhibition. Consistent with the ability to induce EMT, we found that the otherwise negligible migration of *KP* cells was greatly stimulated by TGFβ (Figure S10). Although *KD* cells with LOH of *Smad4*/*Dpc4* (*KD*#1) were capable of wound closure, the process was not appreciably altered by exposure to TGFβ. Wound closure in this setting appeared to be accomplished by proliferation across the gap rather than migration per se, as was evident during close serial monitoring. Moreover, the motility of one *KDD* cell line (*KDD*#2) actually appeared to be inhibited by TGFβ; although these cells continued to proliferate in the presence of TGFβ, they appeared to pile up at the wound's edge rather than spread across the gap (Figure S10). These findings underscore the independent mechanisms modulating proliferation and migration and suggest that *Smad4* signaling contributes substantively to the ability to migrate in response to TGFβ.

Cell-Cycle Mediators Chronicle the Response to TGFβ

To further explore the molecular basis for the cellular behaviors described above, we characterized the time course of expression of several prominent cell-cycle regulators in response to TGFβ. In cells that arrest effectively, we observed both induction of p15^{Ink4b} and prominent levels of p16^{Ink4a} (Figure 6; compare *K*#1, *KP*#1, *KP*#2, and *KDD*#1 with *KD*#1). On the other hand, the absence of either p15^{Ink4b} induction (Figure S9; *KP*#3) or p16^{Ink4a} (*KD*#1) meant unbridled growth. Somewhat surprisingly, the levels of c-*myc* did not change appreciably, for the most part, in response to TGFβ. The dynamic and counterbalancing interplay between TGFβ and the *Myc* proto-oncogene contributes to modulating homeostasis of

Table 1. Cellular and Molecular Responses to TGFβ

Cell Line	Growth Arrest	EMT	Migration	Smad4	Cdk2 Activity	Cdk4 Activity	p15	p16	Myc
KD #1	–	–	–	–	↔	↔	+	–	↔
KDD #1	+	–	–	–	↓	↓	+	+	↓
KDD #2	–	–	–	–	↔	↔	–	–	↓
K #1	+	+	nd	+	↓	↓	+	+	↓
KP #1	+	+	+	+	↓↓	↓	+	+	↓
KP #2	+	+	nd	+	↔	↔	+	+	↔
KP #3	–	+	+	+	↑↑	↔/↑	+	+	↔

Primary pancreatic ductal cells from *K*, *KD*, *KDD*, and *KP* animals were evaluated for the ability of TGFβ to arrest growth, induce EMT, stimulate migration, and affect Cdk2 and Cdk4 kinase activities and levels of myc. The presence or absence of detectable levels of Smad4, p15, and p16 proteins is also noted. ↔, no change; ↑, increased; ↓, decreased.

tissue growth and repair responses in many contexts (Siegel and Massague, 2003). In the primary cell lines studied here, however, c-*myc* levels did not correlate with proliferative state (compare, for example, *K*#1 and *KDD*#2). Interestingly, we did also note that p15^{Ink4b} levels can be induced even in the absence of *Smad4* (see *KDD*#1, Figure 6). Finally, in several cell lines *p21*^{Cip} expression was absent altogether, particularly in the setting of *Trp53* mutation, and in others the levels actually decreased, even in cells that were effectively growth arrested. *p27*^{Kip} expression did not change appreciably over the course of TGFβ exposure (data not shown). Thus, the combined effects of *p15*^{Ink4b} and *p16*^{Ink4a} appeared to be the most potent mediators of growth arrest.

Ultimately, the ability of cells to successfully surmount the G1/S restriction point depends upon the integrated effects of various stimuli and suppressors on the enzymatic activities of the critical cyclin-dependent kinases Cdk4 and Cdk2 (Sherr and Roberts, 2004). Basal Cdk4 kinase activity was modest in general in the cell lines tested and downregulated by TGFβ in some but not in others (Figure 6). A similar, though perhaps even more pronounced profile was observed for Cdk2 activity, which was often robust at baseline. Both Cdk4 and Cdk2 activities were notably decreased in every cell line that experienced significant TGFβ-induced growth inhibition but continued unabated in those cell lines oblivious to the presence of TGFβ. In one *KP* ductal cell line, the kinase activities, Cdk2 in particular, were paradoxically stimulated by TGFβ (Figure S9B). Thus, the ability of TGFβ to modulate proliferation in primary pancreatic ductal carcinoma cell lines is reflected in the coordinated kinase activities of Cdk4 and Cdk2 (summarized in Table 1).

DISCUSSION

Cystic Neoplasms of the Pancreas Provide Alternate Routes to Invasive Carcinomas

Preinvasive neoplasms of the pancreatic ductal epithelium include microscopic PanINs, the most common and best characterized of the precursor lesions, as well as two distinct classes of macroscopic cystic neoplasia, IPMNs and MCNs. Beyond the histological features detailed above, several intriguing clinical criteria further distinguish the two categories of cystic lesions, including anatomic location within the pancreas (central versus peripheral and head versus body and tail), associated symptoms (rare versus common), age at presentation (70–80 years versus 40–50 years), and prevalence by gender (roughly equal versus >10:1 in favor of women) (reviewed in Tanaka et al., 2006). From the limited available knowledge, the critical genetic events underlying the development of these two classes of cystic neoplasms also appear to be distinct (Hruban, 2006). IPMNs have a much lower incidence of mutations in *KRAS* and *TP53* than the PanIN-to-PDA carcinoma sequence and are essentially never found to harbor mutations in *DPC4*/*SMAD4* (Iacobuzio-Donahue et al., 2000a). Approximately one-third of IPMNs carry inactivating mutations in *LKB1*/*STK11*, the gene associated with Peutz-Jeghers syndrome (Sato et al., 2001). A major subset of IPMNs show prominent intestinal differentiation, exhibiting a "villous adenoma" growth pattern and strong expression of intestinal differentiation markers CDX2 and MUC2 (Adsay et al., 2004), which are typically not features of MCNs. IPMNs have also been shown to harbor mutations in *PIK3CA*, a gene often mutated in colon cancer but not PDA (Schonleben et al., 2006). In contrast, the incidence of *KRAS* and *TP53* mutations in MCNs is roughly the same as in PDA, and virtually all (~90%) invasive adenocarcinomas arising in association with an MCN have mutations in *DPC4*/*SMAD4* (Iacobuzio-Donahue et al., 2000b). Thus, mutation of *DPC4* appears to be a distinguishing feature of human mucinous cystadenocarcinomas as compared to IPMNs and their associated carcinomas. Overall, the clinical presentation, biological phenotype, histological appearance, and genetic program of the cystic neoplasms in *KD* and *KDD* animals all strongly resemble human MCNs.

Multiple Modes of TGFβ Signaling Shape the Course of Neoplastic Growth

The TGFβ pathway influences epithelial tumorigenesis by a number of mechanisms, including regulating cell-autonomous effects, modulating immunosurveillance and

escape, and helping to define the nature and extent of stromal interactions with the epithelium (Gorelik and Flavell, 2002; Siegel and Massague, 2003; Bhowmick et al., 2004b). Mutations in a number of critical elements in this pathway have been identified across a range of malignancies. The human aerodigestive tract, and gastrointestinal epithelium in particular, is clearly reliant on an intact pathway to suppress nascent neoplastic growth. Mutations in TGFβ pathway members are frequently encountered in head and neck squamous cell carcinomas, gastric and colorectal cancers, and juvenile polyposis (reviewed in Levy and Hill, 2006). The effects of several of these mutations have been confirmed in animal models (reviewed in Letterio, 2005). Interestingly, targeted mutation of TGFBIIR in fibroblasts alone is sufficient to initiate tumorigenesis in the gastric epithelium (Bhowmick et al., 2004a). Thus, interrupting the dialog on either end between stromal and epithelial cells can loosen the strictures on proliferation and polarity and unravel the architectural integrity of the epithelium.

The frequent mutations in malignancies notwithstanding, the TGFβ pathway is also often complicit in advanced stages of tumorigenesis. Tumor suppressing in certain contexts, tumor promoting in others, TGFβ signaling embodies an inherent duality (Bierie and Moses, 2006). This duality recalls the contrasting roles played by TGFβ in promoting cellular migration and organogenesis during early development, and maintaining checks on unfettered growth in mature organs. A similar dichotomy appears to underlie the distinct features of the two pathogenetic routes to invasive ductal carcinoma described here. Previous studies have elucidated distinctions between Smad-dependent and independent signaling, as well as specific Smad4-dependent and independent effects (for recent examples see Levy and Hill, 2005; Valcourt et al., 2005; reviewed in Derynck and Zhang, 2003). In the primary pancreatic ductal carcinoma cells studied here, both growth inhibition and EMT appeared to require Smad4, and although wound closure was possible in the absence of Smad4, it could be further stimulated by TGFβ in the setting of an intact pathway.

The "canonical" TGFβ pathway involves ligand binding to type I and type II surface receptors; phosphorylation of the receptor Smads, Smad2 and Smad3; and translocation to the nucleus of oligomeric receptor Smad complexes with Smad4, which ultimately effect a context-dependent program of transcriptional activation and repression. More recently it has become clear that this linear conceptualization of a sequential cascade represents an oversimplification of what is, in fact, a complex web of Smad-dependent and independent signaling pathways orchestrated by the TGFβ family of ligands (for reviews see Derynck and Zhang, 2003; Massague et al., 2005). These additional mechanisms of signaling include activation of other pathways by TGFβ, such as MAPK, p38 MAPK, and JNK, as well as effects transduced by distinct combinatorial Smad complexes, and even potentially formation of complexes with other as yet unidentified cofactors. Indeed, constitutive deletion of *Smad2* is not

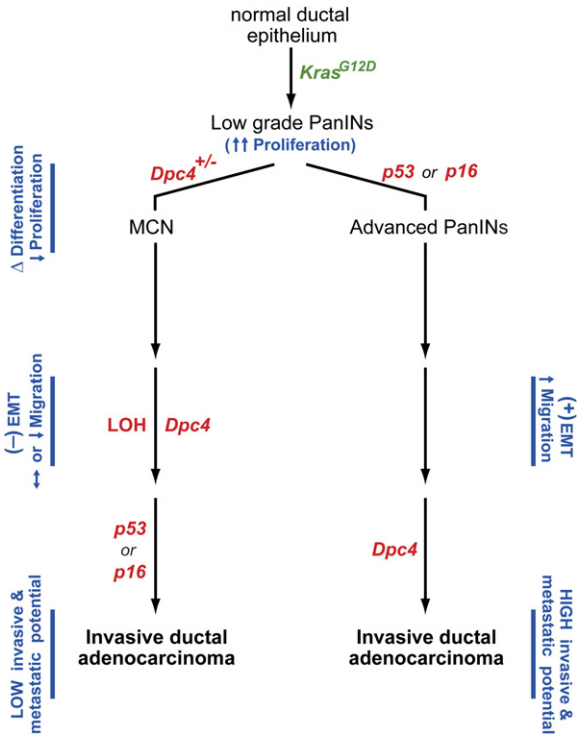

Figure 7. A Model of Divergent Routes to Invasive Ductal Adenocarcinoma of the Pancreas

The timing of specific tumor suppressor gene mutations influences the unique phenotypes and clinical behaviors of invasive ductal carcinomas that arise from MCNs and PanINs, respectively (see text for details).

functionally equivalent to that of *Smad3*, nor is deletion of either receptor *Smad* equivalent to loss of *Smad4* (reviewed in Weinstein et al., 2000). Moreover, in *Smad4* null colon cancer cells, Smad2/3 complexes can nevertheless translocate to the nucleus (Fink et al., 2003). We too have found that TGFβ can induce efficient nuclear translocation of Smad2/3 in *KDD* primary pancreatic ductal cells (data not shown). Thus, the formation of the Smad2/3/4 ternary complex appears to represent only one arm of TGFβ-induced receptor Smad signaling, and both receptor Smads 2 and 3 likely participate in other processes.

Very recently, another candidate for complex formation with Smad2/3 was identified, namely, transcriptional intermediary factor 1γ, or TIF1γ (He et al., 2006). TIF1γ is a nuclear factor that appears to compete with Smad4 for binding to activated Smad2/3 complexes. In erythroid cells, TIF1γ-Smad2/3 complexes mediate TGFβ-induced differentiation, while activated receptor Smads2/3 complexed to Smad4 instead transduce the antiproliferative effects of TGFβ. Thus, TIF1γ, or an analogous protein, would represent an ideal candidate to promote the distinct differentiation program observed in *Smad4*-deficient pancreatic ductal cells in the setting of the proliferative stimulus provided by oncogenic *Kras*^{G12D}, thereby resulting in the elaboration of MCNs as opposed to PanINs. In this

scenario, early loss or deficiency of *Smad4* would tip the balance toward an altered differentiation pattern (i.e., the formation of MCNs), while later mutation of *Smad4* (i.e., after *Trp53*) would no longer be able to affect differentiation, but rather would only serve to remove a remaining impediment to proliferation.

Pathways to Pancreatic Cancer

The collective results of our in vivo and ex vivo experiments suggest a working model that may help reconcile the distinct phenotypic and clinical behaviors of two fundamental routes to invasive ductal adenocarcinoma of the pancreas (Figure 7). Our findings may also help explain how these two disease pathways can share the same overall mutational profile yet portend such dramatically different prognoses for patients. Each route to invasive disease is initiated by oncogenic mutation of *Kras*, which represents the rate-limiting step and results in the formation of early PanIN lesions. Additional mutations in either *Trp53* or *p16* promote progression along the canonical PanIN pathway, resulting in high-grade lesions. On the other hand, we found a relative paucity of advanced PanIN lesions in *KD* animals even as cystic neoplasms began to emerge. We propose that the early-stage PanINs that develop in the setting of concurrent *Kras*^{G12D} expression and *Dpc4* deletion are instead diverted along a distinct differentiation pathway toward cystic neoplasms, concomitant with attenuation of their proliferative rate (we cannot exclude the possibility, however, that the MCNs arise de novo and subsequently suppress PanIN progression by some unknown mechanism). Subsequent LOH of *Dpc4* hastens the progression of these MCNs, while also precluding the development of EMT. Conversely, as the PanINs that progress through mutation of other TSG pathways become invasive, they remain receptive to the induction of EMT and enhanced migration by TGFβ. Subsequent mutation of *Dpc4* at this late juncture in the course of disease progression, as occurs in approximately 55% of human PDA, further unfetters proliferation, resulting in a highly invasive, metastatic, and ultimately lethal disease. Of course, the timing of *Dpc4* mutation may also influence non-cell-autonomous processes, including stromal and immune reactions, which may further contribute to shaping the distinct phenotypic and clinical behaviors of these two pathways to invasive disease.

The model provides a number of readily testable hypotheses. First, if indeed the altered differentiation toward MCNs results from disrupting the balance between Smad4-dependent and -independent signaling pathways, then mutation of components further upstream in the pathway should not engender the same phenotype. In fact, mutations in TGFBRI and TGFBRII have been described (albeit rarely) for classical PDA, but not for MCN-invasive carcinoma. Thus, should concomitant mutation of surface receptors for TGFβ and expression of oncogenic *Kras*^{G12D} result in invasive ductal cancer, we would anticipate a more conventional PDA phenotype. Second, the pathology that ultimately develops in the setting of multiple tumor suppressor gene mutations may reflect the sequence in which the mutations occur in addition to, or even preferentially over, the specific repertoire of mutations. Thus, the model predicts that mutation of *Dpc4*/*Smad4* in the setting of pre-existing or concomitant mutation of either *Trp53* or *p16*^{Ink4a} should result in conventional PDA. Indeed, in preliminary analyses of *Kras*$^{LSL\text{-}G12D/+}$;*Trp53*$^{LSL\text{-}R172H/+}$;*Dpc4*$^{flox/+}$;*Cre* animals, we have observed the development of classical ductal adenocarcinoma of the pancreatic head with glandular histology (D.A.T. and S.R.H., unpublished data), as is seen in *KP* mice (Hingorani et al., 2005). Conversely, as seen in the examples of spontaneous acquisition of *Trp53* or *p16* mutations *after* deletion of *Dpc4* described here, cystic lesions of the body and tail should predominate. This hypothesis also helps explain the loss of *DPC4* expression in virtually all invasive adenocarcinomas in association with MCNs, but only about half of classical ductal adenocarcinomas (in which mutation of *DPC4* is known to occur late in the course of disease progression; Wilentz et al., 2000). Ultimately, this conceptualization implies that even detailed genetic diagnoses of pancreatic cancer subtypes may be strictly insufficient for accurate categorization of tumor type, molecular pathophysiology, and prognosis, as the genetic profile does not reflect the chronology of the mutations. Continuing comparative analyses of the animal models now in hand for these two unique pathways to invasive disease should help further our understanding and management of the challenges they each present.

EXPERIMENTAL PROCEDURES

Mouse Strains

Conditional *Dpc4*$^{flox/+}$ (Yang et al., 2002), *Kras*$^{LSL\text{-}G12D/+}$ (Jackson et al., 2001), and *p48*$^{Cre/+}$ (Kawaguchi et al., 2002) or *Pdx-1-Cre* (kindly provided by Andrew Lowy and described in Hingorani et al. [2003]) strains were interbred to obtain *Kras*$^{LSL\text{-}G12D/+}$;*Dpc4*/*Smad4*$^{flox/+}$;*Pdx-1-Cre* triple mutant animals, as well as *Kras*$^{LSL\text{-}G12D/+}$;*p48*^{Cre} compound mutant, *Kras*$^{LSL\text{-}G12D/+}$;*Dpc4*/*Smad4*$^{flox/+}$;*p48*^{Cre} triple mutant, *Kras*$^{LSL\text{-}G12D/+}$;*Dpc4*/*Smad4*$^{flox/flox}$;*p48*^{Cre} quadruple mutant, and various littermate control animals on a mixed BlSwiss/129/SvJae/C57Bl/6 background. All studies were conducted in compliance with the Fred Hutchinson Cancer Research Center IACUC guidelines.

Histopathology, Immunohistochemistry, Immunoblots, and In Vitro Analyses

Detailed descriptions for these procedures are provided in the Supplemental Data.

Supplemental Data

The Supplemental Data include Supplemental Experimental Procedures, ten supplemental figures, and three supplemental tables and can be found with this article online at http://www.cancercell.org/cgi/content/full/11/3/229/DC1/.

ACKNOWLEDGMENTS

We thank Bethann Pflugeisen for outstanding assistance with figure preparation; Julie Randolph-Habener, Kim Adolphson, and the FHCRC Experimental Histopathology laboratory, as well as Barbara Pruetz, for expert assistance with immunohistochemistry; and Philamer Calses for excellent technical assistance. We are also grateful to Dr. Testuo Sudo for the kind gift of anti-Hes1 antibody. We apologize

to colleagues for our inability to cite many primary references due to space constraints. Supported in part by NCI P50 CA62924 (R.H.H.); NIH R01 CA101973 and NIH U01 CA084291 (D.A.T.); and NCI P30 CA15704, AACR-PanCAN Career Development Award, and the Canary Foundation (S.R.H.).

Received: August 18, 2006
Revised: November 1, 2006
Accepted: January 19, 2007
Published: March 12, 2007

REFERENCES

Adsay, N.V. (2005). Pathological classification of cystic neoplasms of the pancreas. In Pancreatic Cancer, D.D. Von Hoff, D.B. Evans, and R.H. Hruban, eds. (Sudbury, MA: Jones and Bartlett Publishers), pp. 716–756.

Adsay, N.V., Merati, K., Andea, A., Sarkar, F., Hruban, R.H., Wilentz, R.E., Goggins, M., Iocobuzio-Donahue, C., Longnecker, D.S., and Klimstra, D.S. (2002). The dichotomy in the preinvasive neoplasia to invasive carcinoma sequence in the pancreas: Differential expression of MUC1 and MUC2 supports the existence of two separate pathways of carcinogenesis. Mod. Pathol. *15*, 1087–1095.

Adsay, N.V., Merati, K., Basturk, O., Iacobuzio-Donahue, C., Levi, E., Cheng, J.D., Sarkar, F.H., Hruban, R.H., and Klimstra, D.S. (2004). Pathologically and biologically distinct types of epithelium in intraductal papillary mucinous neoplasms: Delineation of an "intestinal" pathway of carcinogenesis in the pancreas. Am. J. Surg. Pathol. *28*, 839–848.

Aguirre, A.J., Bardeesy, N., Sinha, M., Lopez, L., Tuveson, D.A., Horner, J., Redston, M.S., and DePinho, R.A. (2003). Activated Kras and Ink4a/Arf deficiency cooperate to produce metastatic pancreatic ductal adenocarcinoma. Genes Dev. *17*, 3112–3126.

Andea, A., Sarkar, F., and Adsay, V.N. (2003). Clinicopathological correlates of pancreatic intraepithelial neoplasia: A comparative analysis of 82 cases with and 152 cases without pancreatic ductal adenocarcinoma. Mod. Pathol. *16*, 996–1006.

Bardeesy, N., Aguirre, A.J., Chu, G.C., Cheng, K.H., Lopez, L.V., Hezel, A.F., Feng, B., Brennan, C., Weissleder, R., Mahmood, U., et al. (2006). Both p16(Ink4a) and the p19(Arf)-p53 pathway constrain progression of pancreatic adenocarcinoma in the mouse. Proc. Natl. Acad. Sci. USA *103*, 5947–5952.

Bhowmick, N.A., Chytil, A., Plieth, D., Gorska, A.E., Dumont, N., Shappell, S., Washington, M.K., Neilson, E.G., and Moses, H.L. (2004a). TGF-β signaling in fibroblasts modulates the oncogenic potential of adjacent epithelia. Science *303*, 848–851.

Bhowmick, N.A., Neilson, E.G., and Moses, H.L. (2004b). Stromal fibroblasts in cancer initiation and progression. Nature *432*, 332–337.

Bierie, B., and Moses, H.L. (2006). Tumour microenvironment: TGFβ: The molecular Jekyll and Hyde of cancer. Nat. Rev. Cancer *6*, 506–520.

Derynck, R., and Zhang, Y.E. (2003). Smad-dependent and Smad-independent pathways in TGF-β family signalling. Nature *425*, 577–584.

Fernandez-del Castillo, C., Targarona, J., Thayer, S.P., Rattner, D.W., Brugge, W.R., and Warshaw, A.L. (2003). Incidental pancreatic cysts: Clinicopathologic characteristics and comparison with symptomatic patients. Arch. Surg. *138*, 427–433.

Fink, S.P., Mikkola, D., Willson, J.K., and Markowitz, S. (2003). TGF-β-induced nuclear localization of Smad2 and Smad3 in Smad4 null cancer cell lines. Oncogene *22*, 1317–1323.

Gorelik, L., and Flavell, R.A. (2002). Transforming growth factor-β in T-cell biology. Nat. Rev. Immunol. *2*, 46–53.

He, W., Dorn, D.C., Erdjument-Bromage, H., Tempst, P., Moore, M.A., and Massague, J. (2006). Hematopoiesis controlled by distinct TIF1-gamma and Smad4 branches of the TGFβ pathway. Cell *125*, 929–941.

Hingorani, S.R., Petricoin, E.F., Maitra, A., Rajapakse, V., King, C., Jacobetz, M.A., Ross, S., Conrads, T.P., Veenstra, T.D., Hitt, B.A., et al. (2003). Preinvasive and invasive ductal pancreatic cancer and its early detection in the mouse. Cancer Cell *4*, 437–450.

Hingorani, S.R., Wang, L., Multani, A.S., Combs, C., Deramaudt, T.B., Hruban, R.H., Rustgi, A.K., Chang, S., and Tuveson, D.A. (2005). Trp53R172H and KrasG12D cooperate to promote chromosomal instability and widely metastatic pancreatic ductal adenocarcinoma in mice. Cancer Cell *7*, 469–483.

Hruban, R.H. (2006). Tumors of the pancreas. In Atlas of Tumor Pathology, Fourth Series Edition, R.H. Hruban, D.S. Klimstra, and M.B. Pitman, eds. (Washington, DC: Armed Forces Institute of Pathology).

Hruban, R.H., Goggins, M., Parsons, J., and Kern, S.E. (2000). Progression model for pancreatic cancer. Clin. Cancer Res. *6*, 2969–2972.

Hruban, R.H., Iacobuzio-Donahue, C., Wilentz, R.E., Goggins, M., and Kern, S.E. (2001). Molecular pathology of pancreatic cancer. Cancer J. *7*, 251–258.

Hruban, R.H., Takaori, K., Klimstra, D.S., Adsay, N.V., Albores-Saavedra, J., Biankin, A.V., Biankin, S.A., Compton, C., Fukushima, N., Furukawa, T., et al. (2004). An illustrated consensus on the classification of pancreatic intraepithelial neoplasia and intraductal papillary mucinous neoplasms. Am. J. Surg. Pathol. *28*, 977–987.

Hruban, R.H., Adsay, N.V., Albores-Saavedra, J., Anver, M.R., Biankin, A.V., Boivin, G.P., Furth, E.E., Furukawa, T., Klein, A., Klimstra, D.S., et al. (2006). Pathology of genetically engineered mouse models of pancreatic exocrine cancer: Consensus report and recommendations. Cancer Res. *66*, 95–106.

Iacobuzio-Donahue, C.A., Klimstra, D.S., Adsay, N.V., Wilentz, R.E., Argani, P., Sohn, T.A., Yeo, C.J., Cameron, J.L., Kern, S.E., and Hruban, R.H. (2000a). Dpc-4 protein is expressed in virtually all human intraductal papillary mucinous neoplasms of the pancreas: Comparison with conventional ductal adenocarcinomas. Am. J. Pathol. *157*, 755–761.

Iacobuzio-Donahue, C.A., Wilentz, R.E., Argani, P., Yeo, C.J., Cameron, J.L., Kern, S.E., and Hruban, R.H. (2000b). Dpc4 protein in mucinous cystic neoplasms of the pancreas: Frequent loss of expression in invasive carcinomas suggests a role in genetic progression. Am. J. Surg. Pathol. *24*, 1544–1548.

Jackson, E.L., Willis, N., Mercer, K., Bronson, R.T., Crowley, D., Montoya, R., Jacks, T., and Tuveson, D.A. (2001). Analysis of lung tumor initiation and progression using conditional expression of oncogenic K-ras. Genes Dev. *15*, 3243–3248.

Kawaguchi, Y., Cooper, B., Gannon, M., Ray, M., MacDonald, R.J., and Wright, C.V. (2002). The role of the transcriptional regulator Ptf1a in converting intestinal to pancreatic progenitors. Nat. Genet. *32*, 128–134.

Kozuka, S., Sassa, R., Taki, T., Masamoto, K., Nagasawa, S., Saga, S., Hasegawa, K., and Takeuchi, M. (1979). Relation of pancreatic duct hyperplasia to carcinoma. Cancer *43*, 1418–1428.

Leach, S.D. (2004). Mouse models of pancreatic cancer: The fur is finally flying! Cancer Cell *5*, 7–11.

Letterio, J.J. (2005). Disruption of the TGF-β pathway and modeling human cancer in mice. Mutat. Res. *576*, 120–131.

Levy, L., and Hill, C.S. (2005). Smad4 dependency defines two classes of transforming growth factor β (TGF-β) target genes and distinguishes TGF-β-induced epithelial-mesenchymal transition from its antiproliferative and migratory responses. Mol. Cell. Biol. *25*, 8108–8125.

Levy, L., and Hill, C.S. (2006). Alterations in components of the TGF-β superfamily signaling pathways in human cancer. Cytokine Growth Factor Rev. *17*, 41–58.

Maitra, A., Fukushima, N., Takaori, K., and Hruban, R.H. (2005). Precursors to invasive pancreatic cancer. Adv. Anat. Pathol. *12*, 81–91.

Massague, J., Seoane, J., and Wotton, D. (2005). Smad transcription factors. Genes Dev. *19*, 2783–2810.

Offield, M.F., Jetton, T.L., Labosky, P.A., Ray, M., Stein, R.W., Magnuson, M.A., Hogan, B.L., and Wright, C.V. (1996). PDX-1 is required for pancreatic outgrowth and differentiation of the rostral duodenum. Development *122*, 983–995.

Sato, N., Rosty, C., Jansen, M., Fukushima, N., Ueki, T., Yeo, C.J., Cameron, J.L., Iacobuzio-Donahue, C.A., Hruban, R.H., and Goggins, M. (2001). STK11/LKB1 Peutz-Jeghers gene inactivation in intraductal papillary-mucinous neoplasms of the pancreas. Am. J. Pathol. *159*, 2017–2022.

Schonleben, F., Qiu, W., Ciau, N.T., Ho, D.J., Li, X., Allendorf, J.D., Remotti, H.E., and Su, G.H. (2006). PIK3CA mutations in intraductal papillary mucinous neoplasm/carcinoma of the pancreas. Clin. Cancer Res. *12*, 3851–3855.

Sherr, C.J., and Roberts, J.M. (2004). Living with or without cyclins and cyclin-dependent kinases. Genes Dev. *18*, 2699–2711.

Siegel, P.M., and Massague, J. (2003). Cytostatic and apoptotic actions of TGF-β in homeostasis and cancer. Nat. Rev. Cancer *3*, 807–821.

Takaku, K., Oshima, M., Miyoshi, H., Matsui, M., Seldin, M.F., and Taketo, M.M. (1998). Intestinal tumorigenesis in compound mutant mice of both Dpc4 (Smad4) and Apc genes. Cell *92*, 645–656.

Takaku, K., Miyoshi, H., Matsunaga, A., Oshima, M., Sasaki, N., and Taketo, M.M. (1999). Gastric and duodenal polyps in Smad4 (Dpc4) knockout mice. Cancer Res. *59*, 6113–6117.

Tanaka, M., Chari, S., Adsay, V., Fernandez-del Castillo, C., Falconi, M., Shimizu, M., Yamaguchi, K., Yamao, K., and Matsuno, S. (2006). International consensus guidelines for management of intraductal papillary mucinous neoplasms and mucinous cystic neoplasms of the pancreas. Pancreatol. *6*, 17–32.

Thiery, J.P. (2002). Epithelial-mesenchymal transitions in tumour progression. Nat. Rev. Cancer *2*, 442–454.

Valcourt, U., Kowanetz, M., Niimi, H., Heldin, C.H., and Moustakas, A. (2005). TGF-β and the Smad signaling pathway support transcriptomic reprogramming during epithelial-mesenchymal cell transition. Mol. Biol. Cell *16*, 1987–2002.

Warshaw, A.L., and Fernandez-del Castillo, C. (1992). Pancreatic carcinoma. N. Engl. J. Med. *326*, 455–465.

Weinstein, M., Yang, X., and Deng, C. (2000). Functions of mammalian Smad genes as revealed by targeted gene disruption in mice. Cytokine Growth Factor Rev. *11*, 49–58.

Wilentz, R.E., Iacobuzio-Donahue, C.A., Argani, P., McCarthy, D.M., Parsons, J.L., Yeo, C.J., Kern, S.E., and Hruban, R.H. (2000). Loss of expression of Dpc4 in pancreatic intraepithelial neoplasia: Evidence that DPC4 inactivation occurs late in neoplastic progression. Cancer Res. *60*, 2002–2006.

Xu, X., Brodie, S.G., Yang, X., Im, Y.H., Parks, W.T., Chen, L., Zhou, Y.X., Weinstein, M., Kim, S.J., and Deng, C.X. (2000). Haploid loss of the tumor suppressor Smad4/Dpc4 initiates gastric polyposis and cancer in mice. Oncogene *19*, 1868–1874.

Yang, X., Li, C., Herrera, P.L., and Deng, C.X. (2002). Generation of Smad4/Dpc4 conditional knockout mice. Genesis *32*, 80–81.

Zavadil, J., Cermak, L., Soto-Nieves, N., and Bottinger, E.P. (2004). Integration of TGF-β/Smad and Jagged1/Notch signalling in epithelial-to-mesenchymal transition. EMBO J. *23*, 1155–1165.

Zhang, Z., Wang, Y., Vikis, H.G., Johnson, L., Liu, G., Li, J., Anderson, M.W., Sills, R.C., Hong, H.L., Devereux, T.R., et al. (2001). Wildtype Kras2 can inhibit lung carcinogenesis in mice. Nat. Genet. *29*, 25–33.